Role of Histone Tails in the Conformation and Interactions of Nucleosome Core Particles†

Aurélie Bertin,‡ Amélie Leforestier,‡ Dominique Durand,§ and Françoise Livolant*,‡

Laboratoire de Physique des Solides, CNRS UMR 8502, Bât 510, Université Paris-Sud, 91405 Orsay Cedex, and Laboratoire pour l'Utilisation du Rayonnement Electromagnétique (LURE), Bât 209D, Université Paris-Sud, BP34, 91 898 Orsay Cedex

Received December 9, 2003; Revised Manuscript Received February 19, 2004

ABSTRACT: The goal of this work was to test the role of the histone tails in the emergence of attractive interactions between nucleosomes above a critical salt concentration that corresponds to the complete tail extension outside the nucleosome [Mangenot, S., et al (2002) *Biophys. J. 82,* 345−356; Mangenot, S., et al (2002) *Eur. Phys. J. E 7,* 221−231]. Small angle X-ray scattering experiments were performed in parallel with intact and trypsin tail-deleted nucleosomes with 146 ± 3 bp DNA. We varied the monovalent salt concentration from 10 to 300 monovalent salt concentration and followed the evolution of (i) the second virial coefficient that characterizes the interactions between particles and (ii) the conformation of the particle. The attractive interactions do not emerge in the absence of the tails, which validates the proposed hypothesis.

In vitro condensation of chromatin is known to be dependent on the presence of the histone tails of the nucleosome core (for a recent review, see ref *1*). These tails correspond to the N terminal portion of all four histones, and the C terminus of histone H2A. They represent about 30% of the histone mass in the nucleosome, and are highly conserved throughout evolution. They exit out of the nucleosome and are accessible to enzymes such as acetyl tranferases, and methylases, among others. Therefore, they are in position to mediate and control interactions between nucleosomes both along the chain and between chains (*2*−*4*). The major part of histone tails is not resolved in the crystalline structures, suggesting that these tails do not adopt defined positions inside the crystals. It was shown years ago by NMR experiments that the tail domains interact with DNA at low salt and are released and mobile at moderate salt (0.3−0.4 M) (*5*−*8*). Using small angle scattering experiments and well-defined samples, it was shown recently that the extension of the tails occurs at a much lower salt concentration. Their extension is completed at 50 mM monovalent salt for nucleosome core particles (NCP)[1] carrying 146 ± 3 bp DNA, and at a slightly higher salt concentration when the DNA fragment associated with the particle is longer (*9*). By determining the second virial coefficient, the interactions between particles were followed over the same salt range. At low salt, NCPs that are negatively charged interact via net repulsive interactions. Interestingly, the maximal extension of the tails coincides with the emergence of an attraction (*9*). The emergence of an attraction was confirmed by osmometry measurements, and a tail bridging hypothesis was proposed to interpret this effect (*10*). A theoretical investigation confirmed that bridging interactions can be obtained in a system composed of two macroions with two oppositely charged flexible chains, but it was not clear that such effects could lead to a non-monotonic variation of the second virial coefficient as observed with NCPs (*11*).

To test the hypothesis that the tails are responsible for this attraction, we designed a new series of experiments. A batch of nucleosomes was prepared and half of them were treated with trypsin to delete the histone tails. A comparative analysis of the two samples was performed by small angle X-ray scattering to determine whether the deletion of the tails suppressed the attractive interactions between particles. We followed the evolution of the second virial coefficient for monovalent salt concentrations ranging from 10 to 300 mM. The comparison of the intact and tail-deleted NCP clearly shows that the decrease of the second virial coefficient reaches the hard sphere limit for tail-deleted nucleosomes, whereas it decreases below this value for intact NCP. We thus verified that the attractive interactions that emerge between the particles above 50 mM come from the extended tails. We also detected minor effects of the tail-deletion on the conformation of the nucleosome, at moderate salt concentration, that were not reported yet, and become significant at low salt concentration. These effects are discussed here.

MATERIAL AND METHODS

Preparation of Nucleosome Core Particles. NCP were prepared by controlled digestion of H1-depleted calf thymus chromatin with micrococcal nuclease (Pharmacia) as described by Mangenot et al (*9*). The NCPs were suspended in 150 mM NaCl, 10 mM Tris-HCl pH 7.6 and purified by chromatography using Sephacryl S300 HR (Pharmacia). The particles were dialyzed at a concentration of 2 g L^{-1} against

† This work was supported by the CNRS program (ACI Physicochimie de la Matière Complexe).

* To whom correspondence should be addressed. E-mail: livolant@lps.u-psud.fr.

‡ Laboratoire de Physique des Solides, CNRS UMR 8502.

§ Laboratoire pour l'Utilisation du Rayonnement Electromagnétique (LURE).

[1] NCP, nucleosome core particle; aa, amino acids; C_s, monovalent salt concentration; SAXS, small angle X-ray scattering; A_2, second virial coefficient; D_{max}, maximum extension of the particle; R_g, radius of gyration; $P(r)$, distance distribution function; $I(q)$, scattered intensity.

10.1021/bi036210g CCC: $27.50
Published on Web 03/27/2004

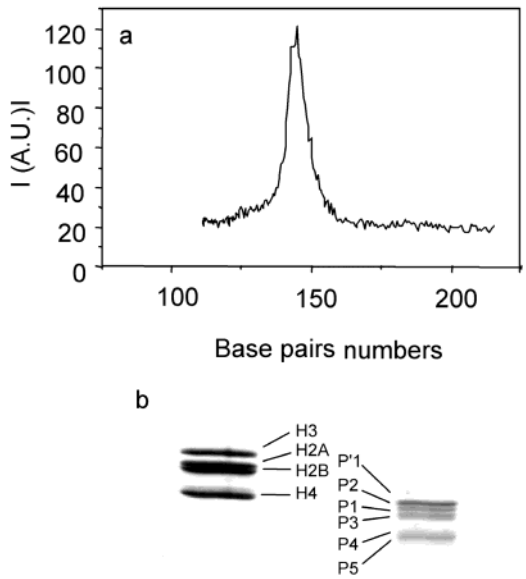

FIGURE 1: Characterization of intact and trypsinized nucleosomes. (a) The distribution profile of DNA fragments lengths (146 ± 3 bp) associated with the histone octamer was determined by scan densitometry of a BET-stained 7.5% polyacrylamide electrophoresis gel. (b) 18% polyacrylamide electrophoresis gel of proteins stained with Coomassie blue. Four bands can be seen, corresponding to the four intact histones H2A, H2B, H3, and H4 (left). For trypsinized NCPs (right), six bands are obtained (P1, P′1, P2, P3, P4, and P5), in agreement with ref *14*.

10 mM Tris-HCl buffer, pH 7.6, and concentrated to 200 g L^{-1} by ultrafiltration in a pressurized cell throughout a hydroxypropylcellulose membrane (Amicon YM100).

Trypsin Digestion of the Histone Tails. Histone tails were digested as described by Ausio et al (*12*), using trypsin attached to agarose beads (TPCK Sigma). Time-course experiments were performed to optimize the enzyme concentration and the digestion time to get the most homogeneous sample. A concentration of 1.3 units of enzyme per mg of NCPs and a digestion time of 7 min 30 s were chosen. Before use, the trypsin beads were washed thoroughly with 25 mM NaCl, 10 mM Tris-HCl buffer, pH 7.6, and drained. The NCPs to be digested were mixed with the suspension of beads at a concentration of 1 g L^{-1} in the same buffer, and the suspension was incubated at room temperature under moderate shaking. Digestion was stopped by the removal of the agarose beads using two 5-min centrifugations at 10 000 rpm, a filtration through a 0.2 μm syringe filter (Millex, Millipore), and finally the addition of an inhibitor of the enzyme (Complete, Roche) at a ratio of 1/100 (v/v). The tail-depleted NCPs were purified by chromatography (Sephacryl S300 HR, Pharmacia) with an elution solution of 10 mM Tris-HCl, 300 mM NaCl, pH 7.6. They were concentrated by ultrafiltration to a concentration of a few mg/mL in the same buffer and stored at 0 °C on ice.

NCP Characterization. After DNA extraction, the length of DNA associated to the histone octamer was assessed at 146 ± 3 bp, by electrophoresis on 12% polyacrylamide gel. The distribution profile of the DNA length associated to the particles is shown in Figure 1a. The absence of any dissociation between histones octamer and DNA was checked by electrophoresis on 7.5% polyacrylamide gel, under nondenaturing conditions. The histone composition of the intact or tail-deleted NCPs was determined using electrophoresis on 18% polyacrylamide SDS gels (Figure 1b). For intact NCPs, four bands of the same intensity indicate that the four histones (H2A, H2B, H3, and H4) are present in stoïchiometric amount. After controlled trypsin digestion, six bands are obtained. Trypsin removes the N-terminal regions of each core histone that extends beyond the edge of the nucleosome, and the shorter but analogous C-terminal tail of histones H2A. According to Böhm et al (*13*−*15*) and to Ausio et al (*12*), the six bands correspond to peptides P′1, P1, P2, P3, P4, and P5. P′1 and P1 correspond respectively to peptides 21−135 (115 aa) and 27−129 (103 aa) of H3; P2 to peptide 12−118 (107 aa) of H2A; P3 to 24−125 (102 aa) of H2B; and P4 and P5 to peptides 18−102 (85 aa) and 20−102 (83 aa) of H4. On top of these six major bands, a few minor ones (seen only when a large amount of material is deposited for electrophoresis) reveal the presence of peptides of higher molecular weight. Using a more sensitive silver staining method (*16*), we determined that the NCPs with incompletely digested tails represent less than 5% of the total number of NCP. This amount was acceptable to perform the proposed SAXS experiments.

The stability of the NCP was checked several times during the experiments, and we detected neither degradation of the histones nor dissociation of DNA from the histone cores.

Sample Preparation. The intact and tail-deleted NCPs solutions were dialyzed against 10 mM Tris-HCl buffer, pH 7.6, containing from 0 to 290 mM NaCl. Both $Tris^+$ and Na^+ ions are included in the total monovalent salt concentration C_s. We investigated C_s concentrations equal to 10, 25, 50, 100, 150, and 300 mM. 0.1 mM PMSF was added in all solutions to prevent degradation of the intact tails or further digestion of the trypsinized particles.

Solutions were concentrated by ultrafiltration to 8 g L^{-1} and the NCP concentration was determined by ultraviolet absorbance at 260 nm using respectively $A_{260} = 9.5$ cm^2 mg^{-1} for intact NCP and $A_{260} = 10.5$ cm^2 mg^{-1} for trypsinized NCP. Samples were further diluted to 4, 2, 1, and 0.5 g L^{-1} by weighing.

Small Angle X-ray Scattering (SAXS) Experiments. The SAXS measurements were carried out on station D24 of the radiation synchrotron source DCI at LURE (Orsay, France). A wavelength of 1.488 Å was selected by a bent germanium monochromator (Ni K-absorption edge). The sample-to-detector distance was 1880 mm. The scattering vector range was $0.01 < q < 0.19$ Å^{-1}, where $q = 4\pi \sin\theta/\lambda$, with 2θ being the scattering angle. The samples were injected in a quartz cell under vacuum. Eight successive frames of 100 s were recorded at room temperature. Buffer was exposed during 16 frames. To improve statistics, the acquisition was repeated two, three, or four times, depending on the NCP concentration. After each acquisition, fresh solution was moved into the beam to be sure that the measurements were not performed on damaged NCPs. No radiation damage was suspected after looking at all frames. The curves were scaled to the transmitted beam before background subtraction.

SAXS Data Analysis. Considering noninteracting particles, the scattering intensity at small q values can be written according to the Guinier approximation (*17*):

$$I(q) = I(0)_{\text{ideal}} \exp\left(-\frac{q^2 R_g^{\,2}}{3}\right) \qquad (1)$$

The intensity at null scattering angle ($q = 0$) is expressed by

$$I(0) = V_{sol}\frac{CM}{N_A}\left(\frac{m_p N_A}{M} - \rho_s \overline{V_p}\right)^2 \quad (2)$$

where C is the NCP concentration (w/v), M the NCP molecular weight, N_A the Avogadro number, m_p the number of electrons in the dry particle, ρ_s the electron density of the buffer, and $\overline{V_p}$ is the partial specific volume of the particle.

R_g is the radius of gyration of the NCP, which can be expressed as follows:

$$R_g^2 = \frac{\int_v r^2 \Delta\rho(r) d^3r}{\int_v \Delta\rho(r) d^3r} \quad (3)$$

For a nearly spherical particle, this approximation can be used when $qR_g < 1.3$. Experimentally, R_g and $I(0)$ are obtained by fitting $\ln(I(q))$ as a function of q^2. Additional information about the particle conformation can be obtained from the distance distribution function $P(r)$ of the particle, which is the Fourier transform of the scattering intensity $I(q)$:

$$P(r) = \frac{r^2}{2\pi^2}\int_0^\infty I(q)\frac{\sin(qr)}{qr} q^2 dq \quad (4)$$

$P(r)$ goes to zero for distances larger than the maximal dimension D_{max} of the particles. $P(r)$ was evaluated using the program GNOM (*18*, *19*). The radius of gyration can also be assessed from the distance distribution function $P(r)$:

$$R_g^2 = \frac{\int_0^{D_{max}} r^2 P(r) dr}{2\int_0^{D_{max}} P(r) dr} \quad (5)$$

For interacting particles, the scattering intensity is modified. It can be expressed as

$$I(q,C) = I(q)_{ideal} S(q,C) \quad (6)$$

$I(q)_{ideal}$ is the scattering intensity in the absence of interactions and is called the form factor. $S(q,C)$ is the structure factor, characterizing the interactions between particles. The scattering intensity at null scattering angle can be expressed as a function of the concentration of the particle C:

$$I(0,C) = \frac{I(0)_{ideal}}{1 + 2MA_2C + 3MA_3C^2 + ...} \quad (7)$$

with M the molecular mass of the particle, A_2 the second virial coefficient that is related to the two particles interactions, and A_3 the third virial coefficient which characterizes the three particles interactions. Considering the particle concentrations used here (0.5−4 mg mL^{-1}), the third virial coefficient can be neglected and the equation above is modified as follows:

$$I(0,C) = \frac{I(0)_{ideal}}{1 + 2MA_2C} \quad (8)$$

A_2 is deduced from the slope of the curve $1/I(0,C)$ as a function of the concentration C. $I(0,C)$ is obtained by the Guinier approximation. The second virial coefficient A_2 simply discriminates between attractive and repulsive interactions. Net repulsive interactions lead to a positive A_2, while attractive interactions correspond to negative A_2 values.

To obtain the form factor $I(q)_{ideal}$ free from interparticle interactions, it is advisable to collect scattering patterns $I(q,C)$ at very low concentration C (e.g., 0.5 mg/mL). In the case of strong interactions, it is even better to extrapolate to zero concentration $I(q,C)$ curves measured at several concentrations C (e.g., 0.5, 1, 2, and 4 mg/mL). Both methods allowed us to obtain an undistorted pattern in the low angle region. In our case, the latter procedure was used only for trypsinized samples at 10 mM where the interactions are strongly repulsive. For the high angle region ($q > 0.05$ Å^{-1}), which is unaffected by interparticle interactions, concentrated solutions (e.g., 4 mg/mL) were used to improve the statistics.

RESULTS

Salt Effects on the Intact and Trypsinized Nucleosome Core Particles. Two series of experiments were performed in parallel, one with intact NCP, and the other with trypsin-digested NCP, prepared from the same batch of nucleosomes.

To follow the shape of the intact NCP, the form factor, $I(q)_{ideal}$ was analyzed for monovalent salt concentrations C_s ranging from 10 to 300 mM. Over the explored salt range, the form factors of intact NCP are similar at high q values ($q > 0.03$ Å^{-1}). Particles keep the same general conformation between 10 and 300 mM monovalent salt concentration. An example is given in Figure 2a for $C_s = 50$ mM. Distance distribution functions were also calculated from the $I(q)_{ideal}$ curves obtained as explained above for the different salt concentrations, using GNOM. Three of them at 10, 50, and 150 mM monovalent salt concentration are presented in Figure 3a. To prevent any effect of interactions at the smallest q values on the $P(r)$ calculations, distribution functions were computed using a q range $q > 0.0217$ Å^{-1}. They are scaled to the intensity at the origin $I(0)$.

For each salt concentration, the maximum extension of the particle D_{max} and the radius of gyration R_g were obtained from the distance distribution function $P(r)$. The radii of gyration obtained from Guinier approximation and from the $P(r)$ curves are not strictly identical but in good agreement, the slight differences remaining within the error bars. As C_s increases, R_g values rise from 42.5 ± 0.5 Å and plateau at a value of 44.5 ± 0.5 Å. This plateau value is reached for $50 \leq C_s \leq 100$ mM (Figure 4a). Simultaneously, the maximal extension of the particle D_{max} goes from 127 ± 5 Å to a plateau value at 147 ± 5 Å (Figure 5a) as noticed on the distance distribution curves (Figure 3a).

After trypsinization of the tails, form factors do not superimpose anymore for high values of the scattering angle ($q > 0.03$ Å^{-1}) at all salt concentrations. For example, the experimental curves recorded at $C_s = 10$ and 50 mM, given in Figure 2b, reveal that the second minimum (at $q = 0.14$ Å^{-1}) is less pronounced at 10 mM. This means that the conformation of the NCP does not remain unchanged over the explored salt range. The values of the radius of gyration R_g decrease from 46 ± 0.5 to 42.5 ± 0.5 Å as the salt concentration increases from 10 to 50 mM and further increase up to 44 ± 0.5 Å at 300 mM (Figure 4b). The

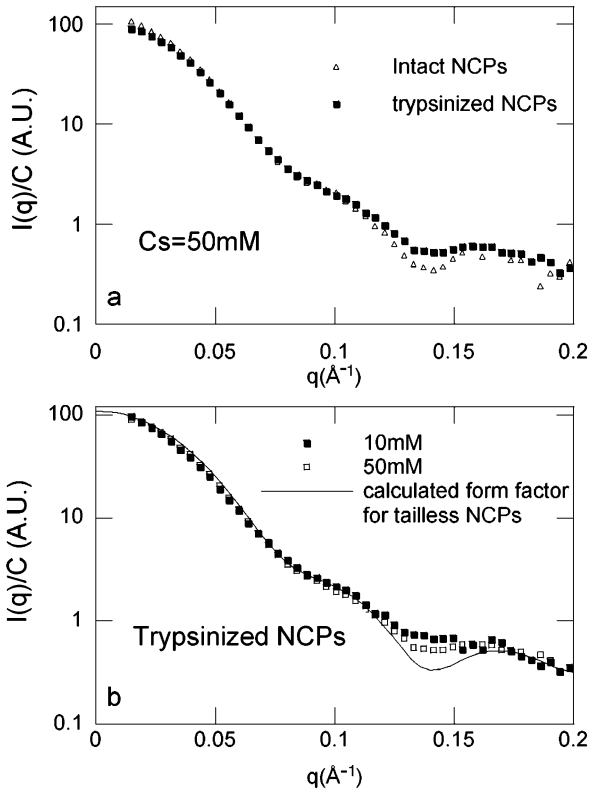

FIGURE 2: Form factors recorded for intact and trypsinized NCPs for different salt concentrations. (a) The form factors for intact (△) and trypsin-digested (■) NCPs do not superimpose for $C_s = 50$ mM. (b) Comparison of the form factors recorded with trysin-digested NCP at $C_s = 10$ mM (■) and $C_s = 50$ mM (□) and calculated for tailless particles (—). The calculated form factor presents a lower second minimum at 0.14 Å^{-1} that is much less pronounced in experimental curves, especially at 10 mM (■). The program CRYSOL (*18*) was used to calculate the scattering intensity, using the PDB file 1eqz from which amino acids belonging to the tails were discarded.

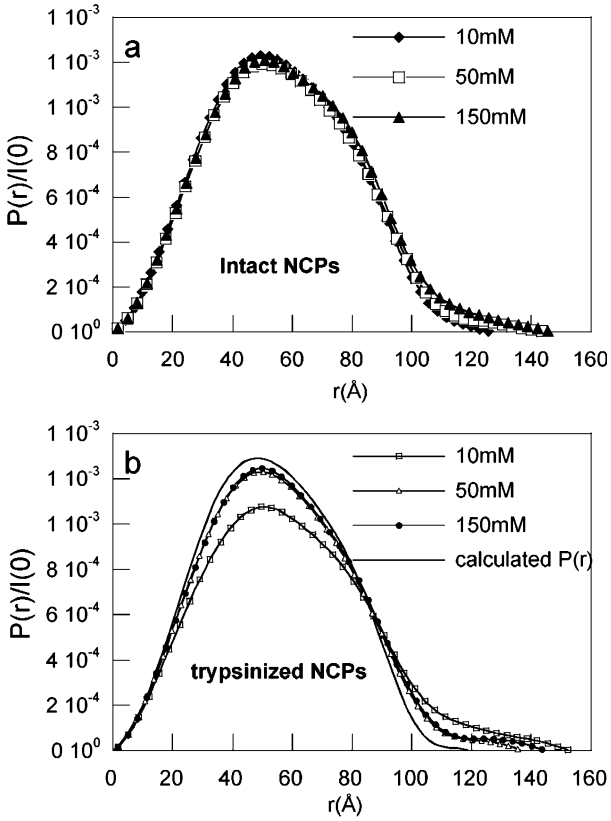

FIGURE 3: Distance distribution functions $P(r)$ obtained for intact (a) and trypsin-digested NCP (b). The curves are scaled to the intensity at the origin $I(0)$. Each $P(r)$ function goes to zero at a distance r that corresponds to the maximum extension of the particle D_{max}. (a) For intact NCP, the $P(r)$ functions recorded at monovalent salt concentrations of 10 (◆), 50 (□), and 150 mM (▲) exhibit similar shapes except for the highest distances. (b) For trypsin-digested NCP, $P(r)$ curves were recorded at 10 (□), 50 (△), and 150 mM (●). The $P(r)$ function was also calculated for a tailless particle using CRYSOL (*18*) and the PDB file 1eqz from which amino acids belonging to the tails were discarded (—). The calculated $P(r)$ leads to a maximal extension value lower than the experimental ones. The curve recorded at 10 mM salt concentration (□) differs significantly from the other curves.

maximal extension of the particle follows the same evolution. It is maximum at 10 mM NaCl ($D_{max} = 154 \pm 5$ Å). It further decreases to 137 ± 5 Å between 25 and 50 mM NaCl and increases again up to 148 ± 5 Å at 300 mM (Figure 5b).

Interactions between Nucleosome Core Particles. For each salt concentration, the scattering profiles were recorded for intact and trypsinized NCP at concentrations of 0.5, 1, 2, and 4 mg/mL NCP. Figure 6a shows the data collected for $C_s = 10$ mM with trypsinized NCPs. The scattered intensity at very low q values decreases when the NCP concentration is raised, which is the signature of repulsive interactions between NCPs. Similar observations were done on intact NCPs. The value of the second virial coefficient A_2 can be derived from these $I(q)$ values, using eq 8 (Figure 6b). A_2 values obtained for both intact and trypsinized NCPs are plotted in Figure 7. For intact NCPs, A_2 values are positive at low salt concentration. They drop when the salinity rises from 10 to 50 mM and become negative above 50 mM. This means that interactions turn from repulsive in the low salt range ($10 < C_s < 50$ mM) to attractive above 50 mM. These observations are consistent with the observations of Mangenot et al (*9*). It can be noticed that at 300 mM, the value of the second virial coefficient is slightly higher, although remaining negative, showing less attractive interactions. For trypsin-digested NCPs, values of the second virial coefficient are positive whatever the salt concentration between 10 and 300 mM. Interactions between trypsin-digested NCPs remain repulsive. More precisely, A_2 decreases from 10 to 50 mM and reaches a plateau above 50 mM. This plateau is very close to the A_2 value calculated for the hard sphere potential of the NCP. The hard sphere value of A_2 is related to the excluded volume and is equal to $4\upsilon NA/M^2 = 4.9 \times 10^{-8}$ mol L g^{-2}, where υ is the volume of the particle.

DISCUSSION

Shape of the Intact NCP. Using intact calf thymus nucleosome cores particles with 146 ± 3 bp DNA, we confirmed the observations of Mangenot et al (*9*) performed with NCP prepared from chicken blood cells, and carrying the same DNA fragment length. When the monovalent salt concentration is raised from 10 to 50 mM monovalent salt, the maximum extension of the particle D_{max} increases progressively. D_{max} further stabilizes at a plateau value above 50 mM. This increase of the maximum extension of the particle was interpreted as a salt-induced change of the conformation of the histone tails. The tails are condensed onto DNA at the periphery of the particle at low salt and they extend outside of the particle when the salt concentration

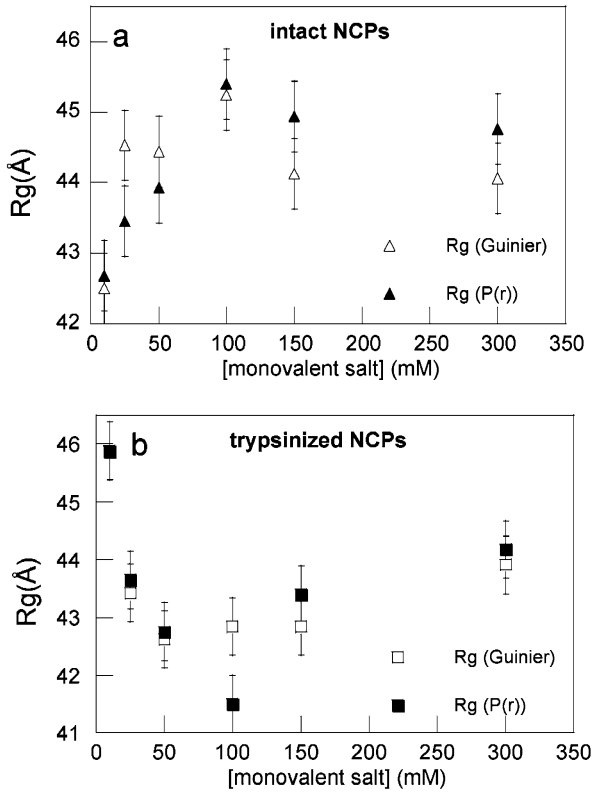

FIGURE 4: Variation of the radius of gyration R_g for intact (a) and trypsinized NCPs (b) as a function of the monovalent salt concentration. Radii of gyration were calculated both by the Guinier approximation (empty symbols) and using $P(r)$ functions (filled symbols). (a) R_g values rise from 42.5 ± 0.5 to 44.5 ± 0.5 Å. (b) For trypsinized NCPs, the values of the radius of gyration R_g decrease from 46 ± 0.5 to 42.5 ± 0.5 Å as the salt concentration increases from 10 to 50 mM and further increase up to 44 ± 0.5 Å at 300 mM.

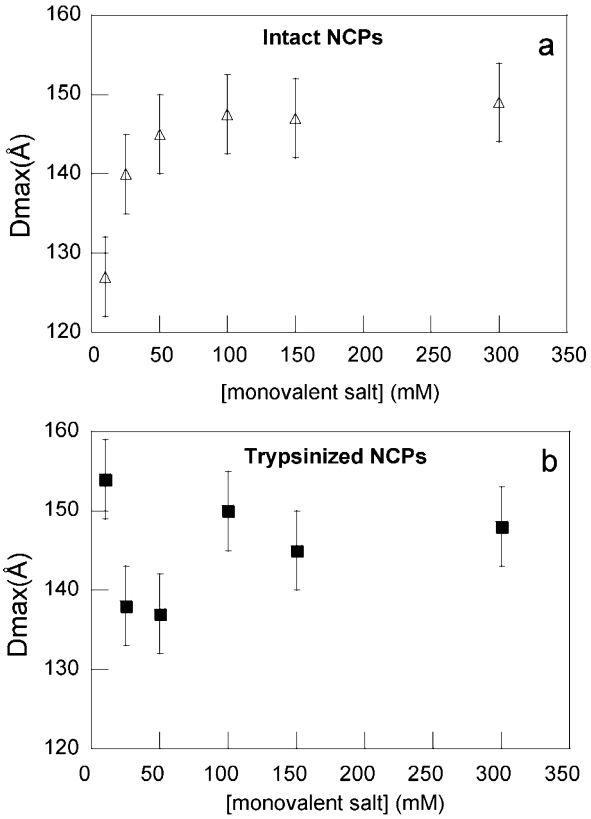

FIGURE 5: Variation of the maximal extension of the particle D_{max} as a function of the monovalent salt concentration for intact (a, △) and trypsinized NCPs (b, ■). (a) For intact NCPs, D_{max} goes from 127 ± 5 to 147 ± 5 Å as the salt concentration increases from 10 to 50 mM. These values plateau between 50 and 300 mM. (b) For trypsinized NCPs, D_{max} is maximum at 10 mM NaCl (D_{max} = 154 ± 5 Å). It further decreases to 137 ± 5 Å between 25 and 50 mM NaCl and increases again up to 148 ± 5 Å at 300 mM.

is increased. As expected, a very small increase of the radius of gyration R_g correlates with this increase of D_{max}. Nevertheless, minor differences can be noticed between the two series of experiments. The maximum extension of the particle increases from 127 ± 5 to 145 ± 5 Å in the present study, from 137 ± 5 to 165 ± 5 Å in the previous one (*9*).

In the previous experiments, we observed a significant increase of the $I(q)$ values, at low q, for increasing NCP concentrations, for salt concentrations $C_s \geq 100$ mM. This effect prevented us from determining the A_2 value for $C_s \geq$ 100 mM. This effect is not observed in the present experiments, suggesting that the purity of the sample was improved. As reported in Mangenot et al (*9*), models of the NCP were built, using the crystallographic coordinates published by Harp et al (2000) (pdb file 1eqz) (*20*) to which the 102 missing amino acids of the tails were added in a random coil configuration. Tools from Turbo-FRODO (*21*) were used to build two models: one with the tails extended away from the particle, in the "extended conformation", and the other with the tails close to the DNA surface, in the "compact conformation". $I(q)$ curves were then calculated for ideal solutions of these two modeled conformations, using the program CRYSOL (*18*). A good fit between calculated and experimental $I(q)$ curves was obtained by placing the tails not too close to the DNA in the compact conformation. In the extended conformation, we observed (see Figure 8 in ref *9*) that the end-to-end distance for a tail containing 25 aa was about 50−55 Å long, slightly more than the expected value (42 Å) for a polypeptide chain with a persistence length of about 10 Å. Considering these new experimental data, the tails are closer to DNA in the compact conformation and not stretched anymore in the extended conformation.

As a conclusion, this new series of experiments confirms our previous observations (*9*) and demonstrates that the conformation of the intact nucleosome slightly changes with the salt concentration. The tails are condensed onto DNA at low salt and extend when the salt concentration is raised. For NCP with 146 bp associated DNA, the extension of the tails is completed at 50 mM, well below the salt concentration at which any change of the NCP conformation had been detected by other methods (for a review, see ref *1*). Moreover, the quality of the data collected in this new series of experiments gave us a more quantitative evaluation of conformational changes. This sample was therefore perfectly suited to test the hypothesis that the extended tails create attractive interactions between the particles.

Salt Dependence of NCP Interactions in Intact and Trypsinized NCP. With intact NCP, the second virial coefficient A_2 varies as described previously (*9*). A_2 values are positive at low salt concentration. These values decrease with the increase of salt concentration, become null at C_s = 50 mM, which corresponds to the full extension of the tails and turn negative above. A small increase of the A_2 values occurs at C_s = 300 mM, although they remain negative. For trypsinized

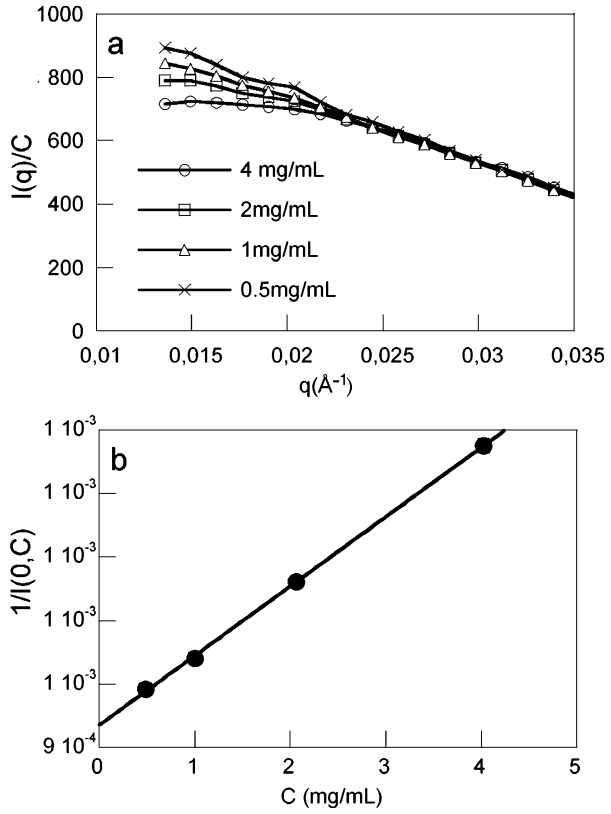

FIGURE 6: Method used to determine the second virial coefficient; example of trypsinized particles at 10 mM monovalent salt concentration. (a) Scattered intensities at small angle values ($q = 4\pi \sin \theta/\lambda < 0.035$ Å^{-1}) are normalized by the particle concentration. The scattered intensity increases when the NCP concentration is lowered, which indicates repulsive interactions between particles in this case. (b) The curve $1/I(0,C)$ as a function of the NCP concentration is a straight line. The slope of this line is related to the second virial coefficient and is equal to $2MA_2/I(0)$ (cf. eq 8).

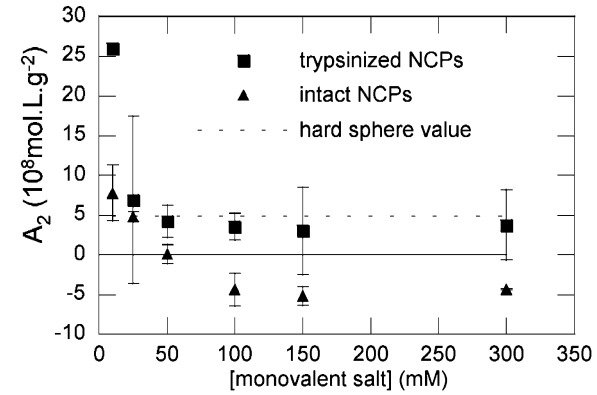

FIGURE 7: Variation of the second virial coefficient as a function of the monovalent salt concentration for intact (▲) and trypsinized (■) NCPs. The dotted line corresponds to the hard sphere value and the continuous line corresponds to the null A_2 value. For intact NCPs, A_2 values are positive at low salt concentration. They drop when the salinity rises from 10 to 50 mM and become negative above 50 mM. For trypsinized NCPs, the second virial coefficient remains positive over all range of salt concentration. A_2 decreases from 10 to 50 mM and reaches a plateau above 50 mM. This plateau is very close to the A_2 value calculated for the hard sphere potential of the NCP.

NCP, the A_2 values also decrease when the salt concentration is raised, and tend to the hard sphere value calculated for tail-deleted NCP. A_2 values remain positive and constant for $C_s \geq 50$ mM. Keeping in mind that negative A_2 values reveal attractive interactions between particles, we conclude that the attractive part of the potential has been suppressed by the elimination of the tails. We thus verified that the attractive part of the potential that exists between the particles above 50 mM comes from the extended tails (*9*, *10*).

The role played by the histone tails in the nucleosome−nucleosome interactions has been explored for years because of its importance in the understanding of chromatin organization. In the presence of monovalent ions (NaCl), reconstituted oligonucleosomes depleted of their tails by trypsinization, remain unfolded upon addition of NaCl and are unable to achieve higher levels of compaction (*22*). Butinelli et al (*23*) also beautifully described how the cooperativity in assembling histone cores onto supercoiled DNA is remarkably decreased after the tails of the octamer histones have been trypsinized, showing that the tails are needed for nucleosomes to attract each other on the supercoiled plasmid DNA. Widlund et al (*24*), using a comparison of histones partitioning between donor histones (either histone cores, mononucleosomes, or long H1-depleted chromatin fragments) to acceptor short DNA fragments of given sequences, also noticed the "unwillingness" of histone octamers to transfer from the oligonucleosome filament to form mononucleosomes. The authors interpret these data as the existence of internucleosomal interactions in chromatin that add to the intranucleosomal interactions between DNA and histones. Furthermore, they showed that these internucleosomal interactions are lost when the histone tails are trypsinized. Similar observations were done in the presence of divalent ($MgCl_2$) cations: trypsinized nucleosomal arrays are also incapable of folding upon addition of 2 mM $MgCl_2$ (*25*). More recently, nucleosome arrays were self-assembled with recombinant, posttranslationally unmodified histone proteins. Upon addition of $MgCl_2$, fully compacted chromatin fibers are obtained with any one of the histone tails deleted, with the exception of the H4 N terminus. More precisely, the amino acids residues 14−19 of H4 contain structural features critical for the formation of the fiber. The importance of this tail was already pointed out from crystallographic studies (*26*).

All these observations were done on nucleosome chains, either linear or circular. To our knowledge, the effect of tail deletion has not been analyzed so far separately from the effect of DNA sequence and topology that have been shown to interfere with tails effects in the emergence of these interactions between NCP (*23*, *24*). Our results clearly establish that in the absence of DNA linking nucleosomes together, histone tails mediate the attractive interactions between NCP above a critical monovalent salt concentration.

Conformation of Trypsinized Nucleosome Core Particles. Trypsinized NCP have been widely used in many laboratories as models of hyperacetylated NCP since the histone extremities cleaved by trypsin carry all the lysine residues that are subject to regulated acetylation in vivo. It is generally accepted that these "tailless" nucleosomes remain otherwise intact in vitro (*12*, *27*−*30*). The ability of X-ray diffraction methods to detect small conformational changes has been demonstrated above with intact nucleosomes. It was therefore tempting to look for possible slight changes of the structure of the nucleosome core introduced by the removal of the tails, possibly undetected yet by less sensitive methods.

In the absence of any crystallographic structure of the tailless nucleosome core particle, the form factor of the NCP deleted from its tails has been calculated, using the crystallographic data published by Harp et al (*20*) from which the amino acids supposedly deleted by trypsin digestion of the tails were removed. The calculated $I(q)$ curve does not fit very well with the experimental curves, whatever the salt concentration is (Figure 2a). The less pronounced minimum in the form factor observed at 0.14 $Å^{-1}$, compared to the calculated curve (Figure 2a) and to the experimental curve of the intact NCP (Figure 2b), reveals that the shape of the particle deviates slightly from the initial cylindrical shape of the NCP. The values calculated for the maximal extension of the particle (D_{max} = 120 Å) and for its radius of gyration (R_g = 41.3 Å) are also notably different from the experimental values (see Figures 4 and 5). It thus appears that the structure of the trypsinized NCP at 50 mM NaCl is slightly different from the crystallographic structure of the intact NCP simply deleted of its tails. The differences are a little more pronounced at 25 mM, and the structure differs significantly from the crystallographic structure at 10 mM. At this salt concentration, the minimum in the form factor almost disappeared and the R_g (45.8 Å) and D_{max} values (153 Å) are far from both the values found experimentally for the intact NCP at the same salt concentration (42.5 and 128 Å, respectively) and the values calculated for the tailless NCP (R_g = 41.3 Å and D_{max} = 120 Å). On account of these structural changes, we may wonder whether trypsin digestion (even under precisely controlled conditions) also introduced other protein cleavages inside the octamer core. The observation of six bands on SDS−PAGE electrophoresis, as already reported by others (*14*), instead of the expected three bands found in reconstituted recombinant tail-deleted reconstituted NCP (*30*) and in trypsinized histones prepared from chromatin fragments (*31*) shows that the tail digestion is not as precise as we would like it to be. Nevertheless, we never observed shorter polypeptide fragments migrating faster than these fragments in gel electrophoresis, even in highly loaded gels, showing that there is no reproducible protein cuts inside the protein core. Moreover, the linearity of Ln(I) as a function of q^2 at low q, attests that the polydispersity is low. Our feeling is that the quality of the samples is as good as we can expect from this trypsinization method, and that the internal structure of the histone octamer is preserved. So, we most likely detected by this low angle scattering method subtle progressive changes of the nucleosome core conformation in the moderate salt concentration range (50−25 mM) that turn significant at 10 mM. Either partial dissociation of the DNA from the histone core or distortions of the core itself could account for such structural changes.

The hypothesis of a partial dissociation of DNA from the histone octamer is supported by theoretical and biological arguments. In the moderate salt range, although structural changes were not described, several observations were done that support the hypothesis of a partial dissociation of DNA from the histone core upon deletion of the tails: (i) The accessibility of DNA for DNAse digestion was increased on 12-mers oligonucleosomes (*22*) as well as on reconstituted isolated nucleosome core particles (*30*); (ii) removal of the tails also leads to a significant but small increase in the position-dependent equilibrium constants for site exposure (*31*) and (iii) reduces the ability of the histone octamer to discriminate between nucleosome positions in reconstitution experiments. The predominant positioning remains the same in the tailless nucleosome, but there is a modestly increased population of alternative positions (*31*). When lowering the salt concentration to 10 mM, this effect is even more important with trysinized NCP and suggests a destructuration of the particle. It can be noticed that intact NCP are also sensitive to such effects at much lower salt concentration (*32*). It can be concluded that the tails are essential to maintain the stability of the NCP to lower salt concentration. To go further in the description of the structural changes that happen at low salt concentration in the presence and in the absence of the tails, there is no doubt that experiments should be performed on recombinant nucleosomes.

As a conclusion, we confirm that for nucleosomes with 146 bp DNA, the salt-induced extension of the histone tails is completed before any other structural change of the nucleosome has occurred, at C_s = 50 mM. The suppression of the tails suppresses the attractive interactions that emerge between NCP above salt concentration for which the histone tails are fully extended. The presence of the tails is therefore necessary for the emergence of this attraction. Nevertheless, the structure of the nucleosome core after trypsin digestion of the tails is not identical to the crystallographic structure of the NCP simply deleted of tails. Further studies should be done with recombinant NCP to establish how the absence of the tails change the structure of the nucleosome core with reference to the structure of the core of the intact NCP, and whether it is possible to discriminate between separate tails effects in these attractive interactions.

ACKNOWLEDGMENT

We thank Eric Raspaud for many fruitful discussions all along this work and Patrice Vachette for assistance in using beamline D24 at LURE.

REFERENCES

1. Zheng, C., and Hayes, J. J. (2003) Structures and interactions of the core histone tail domains. *Biopolymers 68*, 539−546.
2. Schwarz, P. M., Felthauser, A., Fletcher, T. M., and Hansen, J. C. (1996) Reversible oligonucleosome self-association: dependence on divalent cations and core histone tail domains. *Biochemistry 35*, 4009−4015.
3. Widom, J. (1998) Structure, dynamics, and function of chromatin in vitro. *Annu. Rev. Biophys. Biomol. Struct. 27*, 285−327.
4. Wang, X., He, C., Moore, S. C., and Ausio, J. (2001) Effects of histone acetylation on the solubility and folding of the chromatin fiber. *J. Biol. Chem. 276*, 12764−12768.
5. Cary, P., Moss, T., and Bradbury, M. (1978) High-resolution proton-magnetic-resonance studies of chromatin core particles. *Eur. J. Biochem. 89*, 475−482.
6. Walker, I. O. (1984) Differential dissociation of histone tails from core chromatin. *Biochemistry 23*, 5622−5628.
7. Hilliard, P. R., Smith, R. M., and Rill, R. L. (1986) Natural abundance carbon-13 nuclear magnetic resonance studies of histone and DNA dynamics in nucleosome cores. *J. Biol. Chem. 261*, 5992−5998.
8. Smith, R. M., and Rill, R. L. (1989) Mobile histone tails in nucleosomes. *J. Biol. Chem. 264*, 10574−10581.
9. Mangenot, S., Leforestier, A., Vachette, P., Durand, D., and Livolant, F. (2002) Salt-induced conformation and interaction changes of nucleosome core particles. *Biophys. J. 82*, 345−356.
10. Mangenot, S., Raspaud, E., Tribet, C., Belloni, L., and Livolant, F. (2002) Interactions between isolated nucleosome core particles: A tail-bridging effect? *Eur. Phys. J. E 7*, 221−231.

11. Podgornik, R. (2003) Two-body polyelectrolyte-mediated bridging interactions. *J. Chem. Phys. 118*, 11286−11296.
12. Ausio, J., Dong, F., and van Holde, K. E. (1989) Use of selectively trypsinized nucleosome core particles to analyze the role of the histone "tails" in the stabilization of the nucleosome. *J. Mol. Biol. 206*, 451−463.
13. Bohm, L., Briand, G., Sautiere, P., and Crane-Robinson, C. (1981) Proteolytic digestion studies of chromatin core-histone structure. Identification of the limit peptides of histones H3 and H4. *Eur. J. Biochem. 119*, 67−74.
14. Bohm, L., and Crane-Robinson, C. (1984) Proteases as structural probes for chromatin: the domain structure of histones. *Biosci. Rep. 4*, 365−386.
15. Bohm, L., Crane-Robinson, C., and Sautiere, P. (1980) Proteolytic digestion studies of chromatin core-histone structure. Identification of a limit peptide of histone H2A. *Eur. J. Biochem. 106*, 525−530.
16. Merril, C. R. (1990) Silver staining of proteins and DNA. *Nature 343*, 779−780.
17. Guinier, A., and Fournet, G. (1955) *Small Angle Scattering of X-rays*, Wiley, New York.
18. Svergun, D. I., Barberato, C., and Koch, M. H. J. (1995) CRYSOL: a program to evaluate X-ray solution scattering of biological macromolecules from atomic coordinates. *J. Appl. Crystallogr. 28*, 768−773.
19. Svergun, D. I., Semenyuk, A., and Feigin, L. A. (1988) Small-angle scattering angle data treatment by the regularization method. *Acta Crystallogr., Sect. A: Found. Crystallogr. 44*, 244−250.
20. Harp, J. M., Hanson, B. L., Timm, D. E., and Bunick, G. J. (2000) Asymmetries in the nucleosome core particle at 2.5 Å resolution. *Acta Crystallogr., Sect. D: Biol. Crystallogr. 56 Pt 12*, 1513−1534.
21. Roussel, A., and Cambillau, C. (1989) TURBO-FRODO, Silicon Graphics, Mountain View, CA.
22. Garcia-Ramirez, M., Dong, F., and Ausio, J. (1992) Role of the histone "tails" in the folding of oligonucleosomes depleted of histone H1. *J. Biol. Chem. 267*, 19587−19595.
23. Buttinelli, M., Leoni, L., Sampaolese, B., and Savino, M. (1991) Influence of DNA topology and histone tails in nucleosome organization on pBR322 DNA. *Nucleic Acid Res. 19*, 4543−4549.
24. Widlund, H. R., Vitolo, J. M., Thiriet, C., and Hayes, J. J. (2000) DNA sequence-dependent contributions of core histone tails to nucleosome stability: differential effects of acetylation and proteolytic tail removal. *Biochemistry 39*, 3835−3841.
25. Fletcher, T. M., and Hansen, J. C. (1995) Core histone tail domains mediate oligonucleosome folding and nucleosomal DNA organization through distinct molecular mechanisms. *J. Biol. Chem. 270*, 25359−25362.
26. Luger, K., Mader, A. W., Richmond, R. K., Sargent, D. F., and Richmond, T. J. (1997) Crystal structure of the nucleosome core particle at 2.8 Å resolution. *Nature 389*, 251−260.
27. Ausio, J., and van Holde, K. E. (1986) Histone hyperacetylation: its effects on nucleosome conformation and stability. *Biochemistry 25*, 1421−1428.
28. Dumuis-Kervabon, A., Encontre, I., Etienne, G., Jauregui-Adell, J., Mery, J., Mesnier, D., and Parello, J. (1986) A chromatin core particle obtained by selective cleavage of histones by clostripain. *EMBO J. 5*, 1735−1742.
29. Hayes, J. J., Clark, D. J., and Wolffe, A. P. (1991) Histone contributions to the structure of DNA in the nucleosome. *Proc. Natl. Acad. Sci. U.S.A. 88*, 6829−6833.
30. Luger, K., Rechsteiner, T. J., Flaus, A. J., Waye, M. M., and Richmond, T. J. (1997) Characterization of nucleosome core particles containing histone proteins made in bacteria. *J. Mol. Biol. 272*, 301−311.
31. Polach, K. J., Lowary, P. T., and Widom, J. (2000) Effects of core histone tail domains on the equilibrium constants for dynamic DNA site accessibility in nucleosomes. *J. Mol. Biol. 298*, 211−223.
32. Yager, T. D., McMurray, C. T., and van Holde, K. E. (1989) Salt-induced release of DNA from nucleosome core particles. *Biochemistry 28*, 2271−2281.

BI036210G